J. Indian Chem. Soc.,
Vol. 97, No. 9b, September 2020, pp. 1507-1513

Green synthesis, characterization and photocatalytic study of Cu based ZrO_2 nanoparticles

Mithun Kumar Ghosh, Sanjay Kumar Sahu, Debasis Sahoo and Tanmay Kumar Ghorai*

Nanomaterials and Crystal Design Laboratory, Department of Chemistry, Indira Gandhi National Tribal University, Amarkantak-484 887, Madhya Pradesh, India

E-mail: tanmay.ghorai@igntu.ac.in/tanmayghorai66@gmail.com

Manuscript received online 02 July 2020, accepted 29 August 2020

Green synthesis has been adopted for the synthesis of Cu based ZrO_2 nanoparticles via the co-precipitation method. Different mole percentage of copper was incorporated in zirconia and prepare various $Cu_{2x}Zr_{1-x}O_2$ (x = 0.05, 0.1, 0.2, 0.3, 0.4) nanoparticles. Among all the compositions $Cu_{2x}Zr_{1-x}O_2$ (x = 0.05) (CZ) exhibits higher photocatalytic activity compare to pure ZrO_2 and other compositions for degradation of naphthyl orange (NO) under visible light in the aqueous medium. Most interesting that the mol% of Cu^{2+} ion in the mother composition is increased, the degradation rate of NO is decreased but CZ takes only 45 min to decolourize NO completely. The comparative study was also investigated in various model dyes like methyl orange (MO), methyl red (MR), rhodamine B (RhB) including NO in presence of catalysts and oxidation of NO spectra was recorded at constant time interval. CZ nanoparticles were characterized by a host of different techniques such as X-ray diffraction, FTIR, SEM and UV-Visible spectroscopy. The phase structure of $Cu_{2x}Zr_{1-x}O_2$ was cubic and crystallite sizes was found to be 17±1 nm, which was also compatibility from grain sizes of nanoparticles 20±1 nm (SEM analysis). The band gap of $Cu_{2x}Zr_{1-x}O_2$ is 5.03 eV calculated from the optical measurement.

Keywords: Cu based ZrO_2, characterization, nanoparticles, optical and phototocatalytic properties.

Introduction

Water is the basic community to humans, plants and animals. So it is essential that we should always effort to keep it clean. The wastewater is getting to be not kidding natural issues due to their harmfulness and furthermore unsuitable profoundly exceptional shading, exceedingly chemical oxygen demand (COD) content and biological degradation[1].

In recent years, drinking water is a major problem in our world due to slowly increasing population density through mixing wastewater drainage from different dye industries such as textile, pigment, photographic etc.[2–5]. The majority of the dye industries wastewater is containing diverse natural azo colour, which is toxic and these colours are exceptionally harmful in nature and unsafe to sea animals and in addition to the human being[6,7]. Different azo dyes like naphthyl orange, methyl orange, rhodamine B, conga red were the principal material in the dye industry[8–10]. These synthetic colour dyes are pretty and cheap. Therefore the drained water released from industries must purify and it is reused for various purposes of the human being.

Currently number of researchers around the world are working on this area to resolve the issues through expelling unsafe dye from the polluted water by utilizing typical transition metal-based nanoparticles before discharged wastewater to the river or ocean[11–13]. To defeat this issue photocatalytic degradation is a standard protocol or technique amongst other technique to remove organic pollutants from colour dye stuffs[14,15].

In this present work, we emphasize over zirconia-based nanoparticles because of its high surface area, catalytic performance as well as stable, cheap, non-toxic, and it's oxidizing and reducing properties. Therefore, we developed Cu based ZrO_2 nanoparticles by green approach i.e. co-precipitation technique, which is less toxic, environmentally friendly and used as semiconductor-based catalysts. Moreover few articles are reported over the above catalyst. Recently, Kumar *et al.,* reported Cu-ZrO_2 nanocomposite was synthesized by DC method and application study on potentiodynamic polarization and corrosion resistance[16]. After that different group of scientist Cu-ZrO_2 nanocomposites also have been syn-

thesized by ball milling and sol-gel method[17,18].

However, $Cu_{2x}Zr_{1-x}O_2$ (x = 0.05, 0.1, 0.2, 0.3, 0.4) nanoparticles have been successfully synthesis via co-precipitation method and characterized by X-ray diffraction, FTIR, SEM and UV-Visible spectroscopy and study on the photodegradation of NO under sunlight. The novelty of this work is that out of all these compositions, $Cu_{2x}Zr_{1-x}O_2$ (x = 0.05) nanoparticles shows better photocatalytic activity against NO compared to other dyes. It has a cubic structure with crystallite and grain sizes were found 17±1 and 20±1 nm respectively. The band gap of $Cu_{2x}Zr_{1-x}O_2$ is high (5.03 eV), although it behave as semiconductor materials like dimond (5.5 eV)[19]. The $Cu_{2x}Zr_{1-x}O_2$ nanophotocatalysts are eco-friendly, non-toxic, cost-effective and easily synthesized with high yield.

Experimental

Chemicals required:

$Cu(NO_3)_2.5H_2O$ (analytical reagent from SUN CHEM); $ZrO(NO_3)_2.xH_2O$ (analytical reagent from CDH, India); HNO_3, NH_4OH, NO, MO, MR, RhB and *p*-nitrophenol (*p*-NP) (Analytical grade from MERCK, India).

Synthesis:

$Cu_{2x}Zr_{1-x}O_2$ (x = 0.05, 0.1, 0.2, 0.3, 0.4) nanoparticles was synthesised by simple and most demanding co-precipitation technique. Prerequisite amount of $ZrO(NO_3)_2$ and $Cu(NO_3)_2$ were taken according to their composition and were dissolved in the minimum amount of dilute HNO_3 and H_2O in a separate beaker. Now add both the solution and 10 mL of C_2H_5OH was added to the mixture with constant stirring for half an hour until clear the mother solution. After dropwise concentrated NH_4OH was added into the mixture to maintain the pH (8–9) the blue precipitate has appeared. The precipitate was filtered and washed with distilled water for several times until free from alkali. Finally, the precipitate was dried at 200°C for 4 h on the hot air oven and finally collect the fine yellow powder of $Cu_{2x}Zr_{1-x}O_2$ nanoparticles. The colour of zirconia-based nanoparticles are changes with changing the concentration of Cu^{2+} ions. The flow-chart diagram of $Cu_{2x}Zr_{1-x}O_2$ is presented in the following Fig. 1.

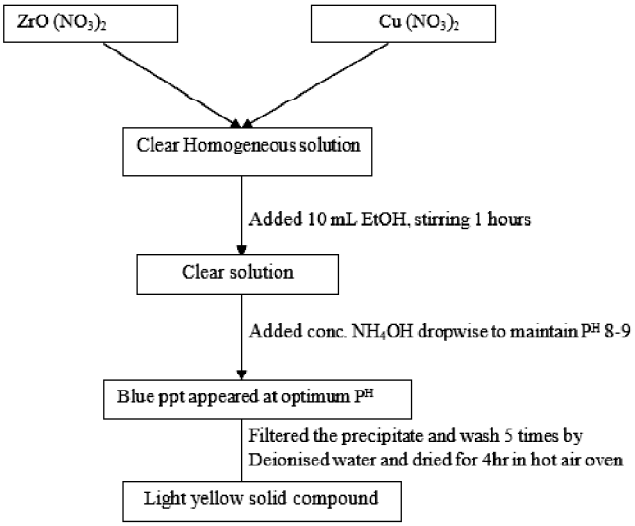

Fig. 1. Flow chart diagram for the synthesis of $Cu_{2x}Zr_{1-x}O_2$ (x = 0.05, 0.1, 0.2, 0.3 and 0.4).

Photocatalytic experiment:

Photocatalytic experiments were conducted using synthesized nanocatalysts, under the aqueous solution of naphthyl orange (NO) and sunlight. The reactions were performed by adding nanopowder of each photocatalyst (0.5 g) into each set of a 20 mL naphthyl orange, which is standardised. Degradation times of naphthyl orange in different time interval as well as compositions were given below. In each set of reactions, solutions are measured by UV-Vis spectrophotometer (UV-1800, Shimadzu) with constant time (10 min) intervals. The maximum absorbance of naphthol orange is at 484 nm.

Characterization:

The crystal structure of $Cu_{2x}Zr_{1-x}O_2$ (x = 0.05) was measured by X-ray diffraction (XRD) at room temperature by using D8 Advance BRUKER, equipped with Cu-Kα (1.54060 Å) as the incident radiation. The Scherrer equation was used for calculation of crystal size. The Scherrer equation was $D = K\lambda/\beta \cos\theta$, $K = 0.9$, D = crystal size (Å), λ = wavelength of Cu-Kα radiation, and β = corrected half-width of the diffraction peak. FTIR-8400S Shimadzu was used for FTIR analysis at room temperature. UV-Visible spectrometer (UV-1800, Shimadzu) was used for the measurement of absorbance. The fine structure of the prepared samples was analysed by Scanning Electronic Microscopy (SEM) (Carl Zeiss Germany, Model Supra-40).

Results and discussion

FTIR spectra analysis:

Fig. 2 represents the FTIR spectrum of $Cu_{2x}Zr_{1-x}O_2$ (x = 0.05) and other compositions (Fig. 2(B)) of the spectral band appears at 527, 565, 1410, 1645 and 3020 cm^{-1}. The two bands observed at 1645 and 3020 cm^{-1} are assigned to stretching vibration of -OH groups due to the absorbed water molecule. The band at 1410 cm^{-1} can be attributed to the absorption of the non-bridging -OH group. The band located near 527 and 565 cm^{-1} can be assigned due to Zr-O and Cu-O stretching mode. All the compositions shows similar spectra and x = 0.05 composition shows better photocatalytic activity therefore we discussed mainly on the characterization of $Cu_{2x}Zr_{1-x}O_2$ (x = 0.05).

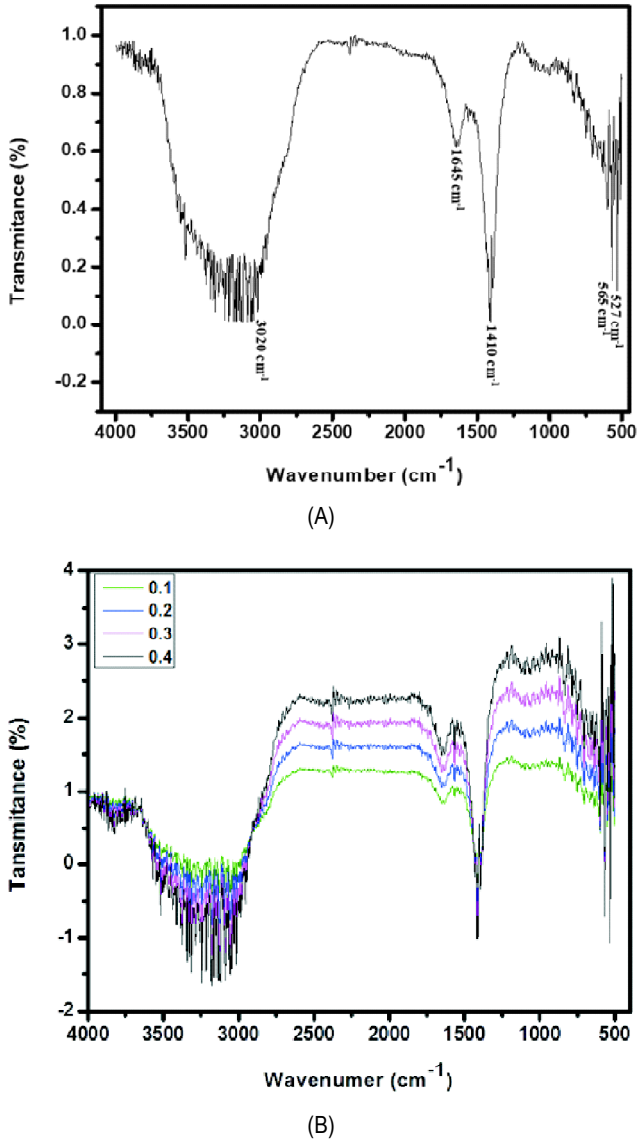

Fig. 2. FTIR spectrum of (A) $Cu_{2x}Zr_{1-x}O_2$ (x = 0.05) and (B) $Cu_{2x}Zr_{1-x}O_2$ (x = 0.1, 0.2, 0.3 and 0.4).

XRD analysis:

The XRD technique was used to determine and confirm the crystal structure of $Cu_{2x}Zr_{1-x}O_2$ (x = 0.05) at 200°C. The intense diffraction peaks observed at 23.02, 32.61, 40.38, 47.02, 52.80, 58.16 and 68.23° were indexed as (110), (111), (305), (220), (300), (311) and (400), respectively (Fig. 3). It indicates the $Cu_{2x}Zr_{1-x}O_2$ has cubic structure with crystalline size is about 17±1 nm measured from the Scherrer equation at (111) plane or maximum intense peak.

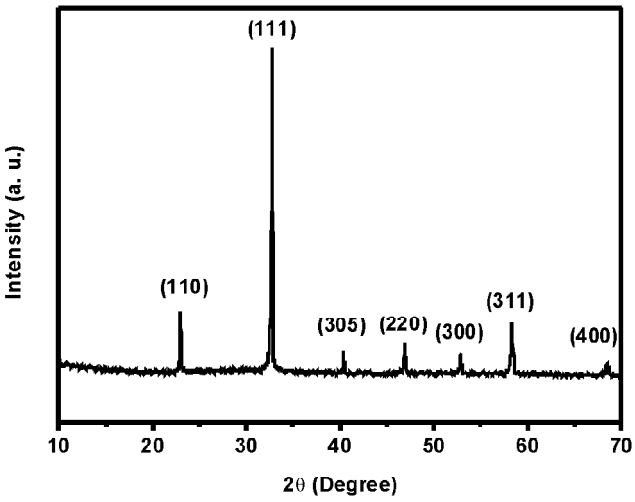

Fig. 3. XRD of $Cu_{2x}Zr_{1-x}O_2$ (x = 0.05).

SEM analysis:

Field Emission Scanning Electron Microscopy (FESEM) is performed to get grain information and surface morphology of the nanoparticles. In Fig. 4 represents the SEM images of $Cu_{2x}Zr_{1-x}O_2$ at x = 0.05 (Fig. 4a-c) and 0.1 (Fig. 4d-f) at different resolutions and they are arranged in a well-ordered manner. Fig. 4a-c has no specific shape but at x = 0.1 (Fig. 4e-f) looks square block shape which is unique.The average grain size of $Cu_{2x}Zr_{1-x}O_2$ is found to be 20±1 nm (Image Tool J). The grain sizes of $Cu_{2x}Zr_{1-x}O_2$ nanoparticles are increased with increasing the mole % of Cu^{2+} (shown in Fig. 4) as a result the catalytic activity of nanoparticles is decreased.

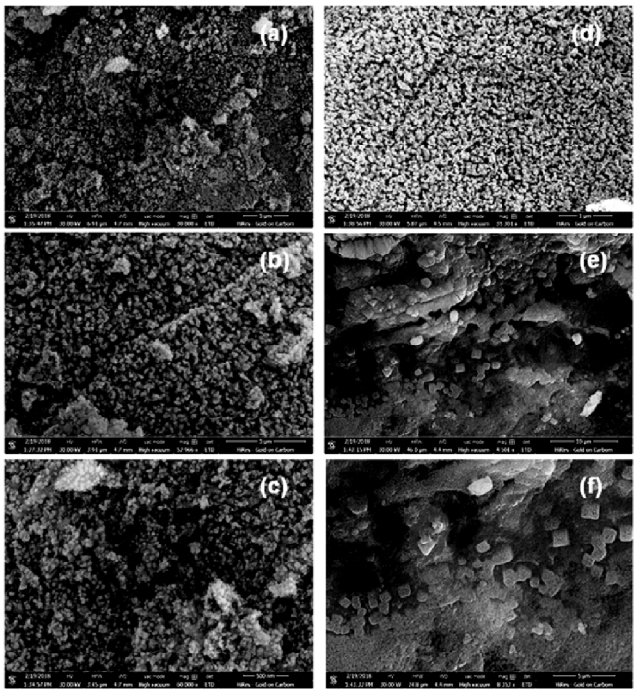

Fig. 4. SEM of CZ (a) $Cu_{2x}Zr_{1-x}O_2$ (x = 0.05)(a-c @ different resolution) and (b) $Cu_{2x}Zr_{1-x}O_2$ (x = 0.1)(d-f @ different resolution).

Photocatalytic activity of $Cu_{2x}Zr_{1-x}O_2$ (CZ):

Photocatalytic experiments were conducted using $Cu_{2x}Zr_{1-x}O_2$ (x = 0.05) (CZ) nanoparticles, different dyes i.e. NO, MB, MO, MR and RhB in aqueous solution and sunlight. The reactions were performed by adding nanocatalyst (0.5 g) into each set of 20 mL of the dye solutions. The significant result was found in presence of NO and $Cu_{2x}Zr_{1-x}O_2$ (x = 0.05), compared to other dyes shown in Fig. 5(a). Fig. 5(b) represents the degradation of NO in presence of $Cu_{2x}Zr_{1-x}O_2$ (x = 0.05) with constant time interval (10 min) and examined by the UV-Vis spectrophotometer. The initial absorbance of NO is about 1.048 at 484 nm and after 45 min the rate of degradation of NO is almost completed and constant upto 85 min. The rate constants (k) of NO in presence of CZ after 45 min is 15.13×10^{-3} min^{-1}. The percentage of degradation of NO, MO, MR and RhB by $Cu_{2x}Zr_{1-x}O_2$ (x = 0.05) was 80.2, 45.5, 12 and 1.9% respectively. The Fig. 6 signify the rate of degradation of naphthol orange in presence of catalysts $Cu_{2x}Zr_{1-x}O_2$ (x = 0.05, 0.1, 0.2, 0.3 and 0.4), ZrO_2 and sunlight. Among all the compositions $Cu_{2x}Zr_{1-x}O_2$ (x = 0.05) shows the highest catalytic activity compared to all other synthesized nanoparticles and ZrO_2. The degradation rate constant of all the nanocatalysts is shown in the following Table 1.

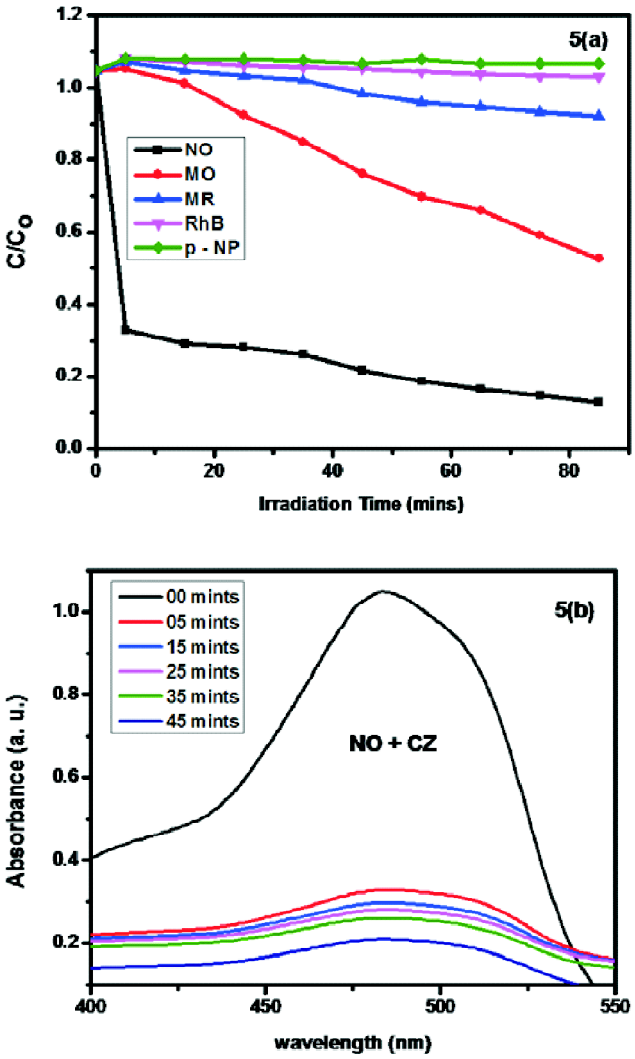

Fig. 5. (a) Degradation of different dye in presence of CZ and sunlight (Top) and (b) UV-Vis spectra of NO in presence of CZ (Bottom).

Table 1

Name of the catalysts $Cu_{2x}Zr_{1-x}O_2$	Reaction rate constant $k(\times10^{-3}$ $min^{-1})$	Crystalline sizes (nm)	Grain sizes (nm)
X = 0.05	15.13	17±1	20±1
X = 0.1	3.06		
X = 0.2	0.06		
X = 0.3	0.005		
X = 0.4	0.001		

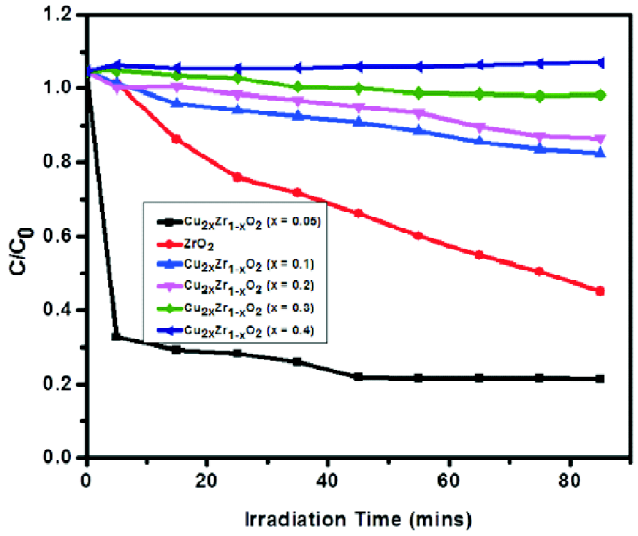

Fig. 6. The rate of degradation of naphthol orange in presence of catalysts $Cu_{2x}Zr_{1-x}O_2$ (x = 0.05, 0.1, 0.2, 0.3 and 0.4) and ZrO_2.

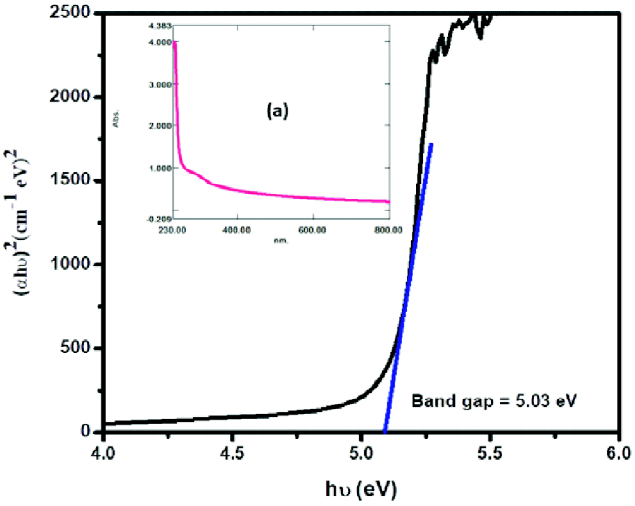

Fig. 7. Band gap energy plot of $Cu_{2x}Zr_{1-x}O_2$ and UV-Visible spectroscopy (inset).

Optical properties:

The solution of $Cu_{2x}Zr_{1-x}O_2$ (x = 0.05) nanoparticles was prepared by a small quantity of water and dil. HCl mixture. The UV spectrum of CZ is shown in inset Fig. 8. We have calculated the energy of the band gap by using Tauc's equation through optical absorption data. Tauc's eq. (1) is shown in the following:

$$(\alpha h\upsilon)^n = A(h\upsilon - E_g) \quad (1)$$

where α denotes the absorption coefficient, h express the Plank's constant, υ is the frequency, A is constant, E_g is band gap and n signify the exponent value and it depends on the type of transition.

The optical energy band gap of $Cu_{2x}Zr_{1-x}O_2$ (x = 0.05) nanoparticle was calculated and found to be 5.03 eV, which shown in Fig. 7.

Proposed mechanism:

In the photocatalytic reaction $Cu_{2x}Zr_{1-x}O_2$ act as a semiconducting materials. The band gap of CuO and ZrO_2 are 1.2 and 3.58 eV[20,21]. The calculated band gap value of $Cu_{2x}Zr_{1-x}O_2$ was 5.03 eV (from optical measurement), which is little bit of high value although it behaves as semiconductor materials like dimond. The oxidation and reduction reaction occurred at the valence and conduction band of the semiconducting material. The proposed photochemical reactions pathway of NO in presence $Cu_{2x}Zr_{1-x}O_2$ is shown in the following equations (Scheme 1).

$$Cu_xZr_{1-x}O_2 + h\nu \longrightarrow e^- (CB) + h^+ (VB) \quad (2)$$

$$O_2 + e^- \longrightarrow O_2^{\bullet -} \quad (3)$$

$$H_2O + h^+ \longrightarrow H^+ + OH^- \quad (4)$$

$$h^+ + H_2O \longrightarrow {}^{\bullet}OH \quad (5)$$

$$NO + h\nu \longrightarrow NO^* \quad (6)$$

$$NO^* \longrightarrow NO^+ + e \quad (7)$$

$$NO^+ + {}^{\bullet}OH \longrightarrow \text{Degradation product} \quad (8)$$

$$NO^+ + O_2^{\bullet -} \longrightarrow \text{Degradation product} \quad (9)$$

Scheme 1. The proposed reaction mechanism for degradation of the NO in the presence of nanoparticles and sunlight.

In presence of sunlight, $Cu_{2x}Zr_{1-x}O_2$ nanoparticles absorb the photon and prompt to produced electron or hole (e^-/h^+) pair demonstrated in (eq. (2)). Naphthyl orange (NO) adsorbed onto the surface of nanocatalysts and the catalytic reaction is going on to the surface of catalysts. The photoelectron which is generated in the conduction band of $Cu_{2x}Zr_{1-x}O_2$ interact oxygen molecules to formed superoxide radicals ($O_2^{\bullet -}$) (eq. (3)). The holes which are formed in valence band in $Cu_{2x}Zr_{1-x}O_2$ which react with a water mol-

ecule to produced hydrogen ion and hydroxyl anion (eq. (4)) and further it can lead to dissociated of water molecules to produced highly active hydroxyl radicals (•OH) (eq. (5)). On the other side, NO is activated by absorbing sunlight and produced NO* (eq. (6)) and NO* released electron and produced NO^+ (eq. (7)). NO^+ react with highly activated hydroxyl radicals (•OH) and superoxide radicals ($O_2^{\bullet-}$) and degradation of the dye (eqs. (8) and (9))[18]. The schematic proposed mechanism is also shown in the model picture (Fig. 8).

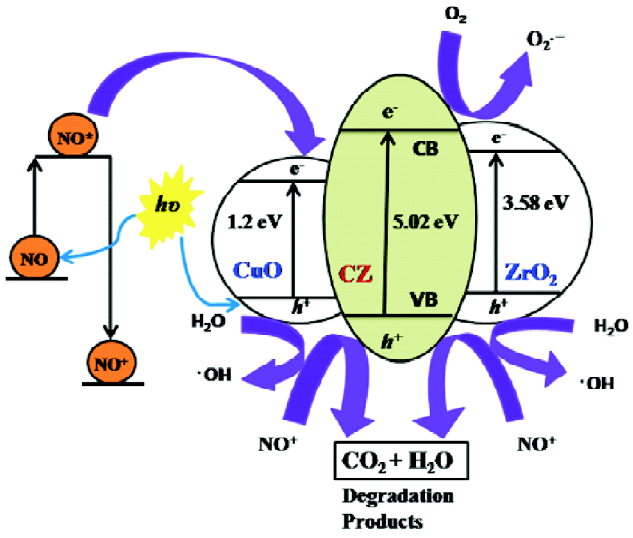

Fig. 8. Schematic proposed mechanism of NO by $Cu_{2x}Zr_{1-x}O_2$ in presence of sunlight.

Conclusion

In summary, we report the synthesis of nano $Cu_{2x}Zr_{1-x}O_2$ (x = 0.05–0.5) catalysts by the green method. It is effectively oxidised naphthyl orange and releases its toxic activity. The $Cu_{2x}Zr_{1-x}O_2$ (x = 0.05) has the highest catalytic efficiency among all the other prepared nanoparticles and takes only 45 min to decolourize NO completely. Photocatalytic degradation of NO in presence of sunlight was rationalized by the production of photo-induced hole-electron pairs in presence of $Cu_{2x}Zr_{1-x}O_2$ (x = 0.05) nanoparticles which would react with dissolved oxygen leading to break down of the azo dye structure giving graded products such as CO_2 and H_2O. Interestingly, in the composition, Zr concentration (9.5 mol%) is high and the Cu concentration (0.05 mol%) is minimum the photocatalytic efficiency of $Cu_{2x}Zr_{1-x}O_2$ (x = 0.05) acquire maximum in presence of NO and sunlight and its optical band gap value is 5.03 eV. The phase structure of $Cu_{2x}Zr_{1-x}O_2$ was cubic and crystallite sizes were found to be 17±1 nm, which was also compatibility from grain sizes of SEM analysis of nanoparticles i.e. 20±1 nm. The catalytic activity in a different type of organic reaction and antimicrobial activity will be studied in further work.

Acknowledgement

This work was fully supported by Madhya Pradesh Council of Science and Technology, Govt. of India, Madhya Pradesh (File No. A/R&D/RP-2/Phy. & Engg./2017-18/271) and Indira Gandhi National Tribal University, Amarkantak, Madhya Pradesh, India. Author's also thankful to Dr. Hari Singh Gour University (Central University), Madhya Pradesh, India for measurement of XRD, SEM and FTIR.

References

1. Y. Jing, L. Li, Q, Zhang, P. Lu, P. Liu and X, Lü, *J. Hazard. Mater.*, 2011, **189**, 40.
2. M. K. Ghosh, K. Jain, S. Khan, K. Das and T. K. Ghorai, *ACS omega*, 2020, **5**, 4973.
3. G. Herrera and N. Montoya, *PhysChemChemPhys*, 2013, **15**, 19312.
4. World Health Organization, Guidelines for drinking-water quality (2008), WHO, Third Edition Incorporating the First and Second Ammenda, Geneva, Vol. 1.
5. US Environmental Protection Agency (1998), Microbial and disinfection by product rules, Federal Register 63:69389.
6. T. K. Ghorai, M. Chakraborty and P. Pramanik, *J. Alloys Compd.*, 2011, **509**, 8158.
7. D. Wang, Y. Duan, Q, Luo, X. Li, J. An, L. Bao and L. Shi, *J. Mater. Chem.*, 2012, **22**, 4847.
8. N. Daneshvar, D. Salari and A. R. Khataee, *J. Photochem. Photobiol. A: Chem.*, 2004, **162**, 317.
9. B. J. Brüschweiler and C. Merlot, *Regul. Toxicol. Pharm.*, 2017, **88**, 214.
10. D. Rawat, V. Mishra and R. S. Sharma, *Chemosphere*, 2016, **155**, 591.
11. M. Zhang, C. Shao, Z. Guo, Z. Zhang, J. Mu, P. Zhang, T. Cao and Y. Liu, *ACS Appl. Mater. Interfaces.*, 2011, **3**, 2573.
12. D. H. Wang, L. Jia, X. L. Wu, L. Q. Lu and A. W. Xu, *Nanoscale*, 2012, **4**, 576.
13. D. Binding and F. Steinbach, *Nature*, 1970, **227**, 832.
14. Z. Zhang, Y. Yu and P. Wang, *ACS Appl. Mater Interfaces*,

2012, **4**, 990.

15. P. K. Sanoop, S. Anas, S. Ananthakumar, V. Gunasekar, R. Saravanan and V. Ponnusami, *Arab. J. Chem.*, 2016, **9**, S1618.
16. K. A. Kumar, A. Sakthivel, A. Vijayakumar, A. Sarathi and S. Senthilkumar, *J. Adv. Appl. Sci. Res.*, 2017, **1**, 54.
17. A. Fathy, A. Wagih and A. Abu-Oqail, *Ceram. Int.*, 2019, **45**, 2319.
18. T. Sreethawong, S. Ngamsinlapasathian and S. Yoshikawa, *Chem. Eng. J.*, 2013, **228**, 256.
19. Kittel, Charles. Introduction to Solid State Physics, 7th Edition, Wiley.
20. J. Li, X. Jin, R. Li, Y. Zhao, X. Wang, X. Liu and H. Jiao, *Appl. Catal. B: Environ.*, 2019, **240**, 1.
21. S. N. Basahel, T. T. Ali, M. Mokhtar and K. Narasimharao, *Nanoscale Res. Lett.,* 2015, **10**, 73.